https://doi.org/10.1016/j.renene.2020.09.027

Modelling analyses of the thermal property and heat transfer performance of a novel compositive PV vacuum glazing

Junchao Huang [a], Xi Chen [a,b*], Jinqing Peng [c], Hongxing Yang [a**]

[a] *Renewable Energy Research Group (RERG), Department of Building Services Engineering, The Hong Kong Polytechnic University, Hong Kong, China*

[b] *School of Science and Technology, The Open University of Hong Kong*

[c] *College of Civil Engineering, Hunan University, Changsha 410082, China*

Abstract

This paper proposes an integrated photovoltaic vacuum glazing unit with an intermediate air cavity and a calibrated modelling approach to quantify its thermal properties and evaluate the heat transfer performance. Theoretical analyses of the heat transfer process are conducted with reasonable hypotheses and traceable boundary conditions. Three-dimensional heat transfer models are then established and cross-validated against previous publications. The detailed validation demonstrates the reliability of the developed complex models under different circumstances. Furthermore, four photovoltaic vacuum glazing configurations are compared in terms of the temperature distribution and overall heat transfer coefficient (i.e. U-value). Simulation results show that the photovoltaic vacuum double glazing can achieve the optimum performance among the four configurations based on simultaneous consideration of the PV module temperature and U-value. Sensitivity analyses of glazing design factors are also conducted for the U-value, which is found to be greatly reduced by decreasing the density and diameter of vacuum pillars as well as the glass thermal conductivity. A lowest U-value of 0.23 W/(m^2·K) is achieved for the photovoltaic-vacuum double glazing and can be further improved with future design optimizations. This research can provide guidance to design improvement of PV vacuum glazing systems and promote their integration with building modelling tools.

Keywords: *Photovoltaic vacuum glazing; Thermal property; Heat transfer; Temperature distribution; U-value*

Nomenclature

Abbreviation

Corresponding authors:
*climber027@gmail.com; pchen@ouhk.edu.hk
**hongxing-yang@polyu.edu.hk

PVLG	photovoltaic laminated glazing: glass-PV layer-glass
PVDG	photovoltaic double glazing: glass-PV layer-glass-air cavity-glass
VG	vacuum glazing: glass-vacuum pillars-glass
TVG	triple vacuum glazing: glass-vacuum pillars-glass-vacuum pillars-glass
EVA	ethylene-vinyl acetate
PV-VG	umbrella name for all kinds of photovoltaic-vacuum glazing
VPVG	vacuum photovoltaic glazing: outdoor/vacuum glazing-PV layer-glass/indoor
VPVDG	vacuum photovoltaic double glazing: outdoor/vacuum glazing-air cavity-glass-PV layer-glass/indoor
PVVG	photovoltaic vacuum glazing: outdoor/glass-PV layer-vacuum glazing/indoor
PVVDG	photovoltaic vacuum double glazing: outdoor/glass-PV layer-glass-air cavity-vacuum glazing/indoor

Symbols		*d*	diameter
η	energy conversion efficiency	*H*	height
α	temperature coefficient		
T	temperature	*Subscripts*	
q	heat flux	*c*	solar cell
T_{ext}	temperature of the external fluid	*std*	standard condition
k	thermal conductivity	*glazing*	glazing layers
h	heat transfer coefficient	*g*	glass
R	thermal resistance	*p*	vacuum pillar
Q_{int}	heat flux on internal surface	*in*	indoor
A	area	*out*	outdoor
U	overall heat transfer coefficient	*cond*	conduction
t	thickness	*conv*	convection
ε	emissivity	*rad*	radiation
s	separation		

1 Introduction

As the contact with the outside world for building occupants, windows bring daylight and passive heating/cooling, but can also give rise to the building energy load and glare issue. Compared with other parts of the building envelope, windows are more likely to cause heat gain in summer and heat dissipation in winter because of their relatively high overall heat transfer

coefficient (i.e. U-value) [1]. Hence, advanced glazing technologies with lower U-values are preferred to limit the heat transfer through the envelope. Cuce and B. Riffat concluded that many kinds of novel glazing had been investigated and developed by means of structural improvement, material replacement and technological innovation although double glazing still dominated the market [1]. Typical innovative glazing includes multilayer glazing, vacuum glazing, photovoltaic glazing, aerogel glazing and so on. For the multilayer glazing, integrating glazing layers (e.g. triple glazing layers) with gases (e.g. 12mm Krypton gap) could lower the U-value to 0.49 W/m^{2}K. Vacuum glazing with a narrow vacuum chamber supported by an array of vacuum pillars can further minimize the conductive and convective heat transfer between two layers of glass [2], and therefore presents a promising window structure to decrease the U-value. In addition to the traditional vacuum glazing that contains only two layers of glass, hybrid vacuum glazing with an air cavity and triple vacuum glazing with two vacuum chambers can achieve better thermal insulation performances [3]. Moreover, the photovoltaic glazing technology, using the ethylene vinyl acetate (EVA) to sandwich solar cells between two sheets of glass, has promising advantages as alternative envelope materials in generating electricity, adjusting daylight [4] and reducing building energy demands [5,6]. It offers an excellent solution to apply renewable energy technologies to building envelopes. PV glazing can be divided into four categories according to the type of embedded solar cells: silicon-based, thin-film, dye-sensitized and organic [7].

However, traditional photovoltaic glazing is usually criticized for its relatively high U-value [8], which is not ideal for thermal insulation and incurs more heating and cooling loads. As inefficient glazing accounts for about 30% of extra heating and cooling energy consumption [9], the thermal performance of photovoltaic glazing becomes especially important. In order to improve the thermal performance of conventional photovoltaic laminated glazing (PVLG), an air cavity is integrated to construct photovoltaic double glazing (PVDG), whose U-value is reduced but still higher than expected. It has been reported that even two layers of Low-E coatings cannot reduce the U-value below 2.4 W/(m^2·K) [10], although the emissivity is as low as 0.05. Given that Low-E coatings are still inefficient in reducing the heat transfer through PVDG. As for the other type of advanced glazing technologies, vacuum glazing (VG) has been widely explored for enhanced thermal insulation performances. The U-value of VG can reach 0.80 W/(m^2·K) at the center area with two layers of Low-E coatings [3]. Triple vacuum glazing (TVG) can further lower the U-value at the center glazing area to 0.22 W/(m^2·K) [11]. This ideal U-value was obtained with four Low-E coating layers with an emittance of 0.03 in two vacuum chambers of triple vacuum glazing. The glass sheets are 4mm thick and the stainless-steel pillars are 0.2mm high with a radius of 0.15 mm and spacing of 25mm.

Given the excellent thermal insulation performance of VG, some researchers have proposed to combine photovoltaic glazing with VG, aiming at improving the thermal performance of BIPV applications and related building energy performances. Photovoltaic glazing was simply coupled with vacuum glazing by a layer of polyvinyl butyral [8], making up a 1300 mm (width) × 1100 mm (height) × 20.87 mm (thickness), a-Si based PV double glazed insulating glass units. Our research group also determined the electrical performance of the structure under standard test conditions, i.e. solar radiation 1000 W/m^2, solar cell temperature 25 ℃, and air mass 1.5). The open-circuit voltage was 120 V, the short circuit current was 0.98 A and the module efficiency was 5.2%. Outdoor experiments were done and results proved that combining PV laminate and vacuum glazing can help reduce heat gain. Later on, tested a similar sample with a smaller size (300 × 300 × 21 mm^3) using a hot box, and the composite glazing achieved a U-value of 1.5 W/(m^2·K) [12]. Sensitivity analyses are conducted for a higher-rise office building with PV vacuum glazing and passive architectural design [13]. The study indicates that a maximum building energy saving of 61% can be achieved in cold areas by optimizing design factors such as the building orientation, window U-value, window to wall ratio, and visible transmittance. A following work developed an artificial neural network model to predict the indoor illuminance for CdTe-based PV vacuum glazing [14], presenting a new solution for accurately calculating the lighting consumption. A study on the applicability of such novel PV vacuum glazing to five major climatic zones of China has also been conducted [15]. The novel glazing is proved to save more than 43% building energy in heating-dominated areas and 35% in cooling dominated areas, but could cause undesired cooling load in the moderate climate.

Another structure of multicrystalline silicon based PV vacuum glazing (PV-VG) with three layers of glass achieved a U-value of 0.8 W/(m^2·K) [16], no matter whether the PV layer faces indoor or outdoor. The U-value was determined using a 0.37 m × 0.22 m × 0.26 m test cell under incident radiation from an indoor solar simulator. Surface temperatures were also measured and a higher surface temperature difference was found in PV vacuum glazing than PV double-glazing. The study also presents a numerical heat transfer model to investigate the thermal performance, indicating a 39% improvement of indoor thermal comfort when using such PV-VG in UK as compared with photovoltaic glazing [17]. It is suggested that solar cells should face the indoor environment in UK while facing the outdoor environment in India. Furthermore, the glazing factor and color properties of PV vacuum glazing are also analyzed in their work [18]. A lower U-value of 0.6 W/(m^2·K) is measured in an a-Si thin film based PV vacuum glazing utilizing the calibrated hot box [19], and a thinner type of PV vacuum glazing containing only two sheets of glass is further tested and numerically investigated [20]. In their study, the aerogel pillar is proved to have an

extraordinary thermal conductivity of 0.032 W/mK with a radius of 0.5 mm, height of 0.3 mm and spacing of 47mm. Compared with conventional stainless-steel pillars, aerogel pillars can additionally decrease 20% of the U-value. Base on the above detailed review of limited existing research on composite PV vacuum glazing, it can be found that thermal modeling is mostly restricted to the one-dimensional heat flux assumption [17,19,20].

Apart from the U-value, the PV module temperature is another point worth investigation. It is known that the power generation performance of a PV module varies inversely with its temperature. Park et al. pointed out that generated electricity dropped by about 0.5% with 1℃ temperature rise through experimental studies under both the approximate standard test condition and real outdoor condition [21]. It is also mentioned that a lower temperature of the PV module contributes to more power outputs when connected to a cold environment rather than vacuum glazing [16]. The photovoltaic glazing energy conversion efficiency changes with the temperature of the PV module as per Eq. (1) [22]:

$$\eta_c = \eta_{std} - \alpha\left(T_c - T_{c,std}\right) \quad (1)$$

where η_c is the PV module's energy conversion efficiency at the temperature of T_c; η_{std} is the efficiency at $T_{c,std}$, the standard condition; and α is the temperature coefficient.

Given the impact on the electricity generation [21,23], the temperature of the PV module is a critical parameter to assess its application potential. Furthermore, the internal surface (in contact with the indoor environment) temperature of photovoltaic glazing can influence the resultant cooling or heating load. A smaller difference between this temperature and the indoor ambient temperature can lead to less convective and radiative heat exchange as well as indoor thermal discomfort [24]. The temperature difference between the outdoor and indoor environment is therefore an essential performance index as measured by the overall heat transfer coefficient (i.e. U-value).

From the above literature review, PV-VG may contain two to four layers of glass depending on different configurations while detailed sensitivity analyses on its thermal performance against different design factors have not yet been thoroughly explored by researchers. Therefore, this paper firstly proposes a novel prototype glazing system integrating PV glazing and vacuum glazing by an air cavity, which is named after VPVDG or PVVDG depending on the relative location of the PV module and vacuum glazing (See Fig. 1). Together with the discussed PV-VG containing three layers of glass [16], the thermal property and U-value are quantified and evaluated by a modelling approach using COMSOL Multiphysics [25]. Furthermore, the impact of critical design factors on the U-value of compositive PV vacuum glazing is extensively analyzed and discussed. In the following part of this paper, Section 2 analyzes the theoretical heat transfer process and elaborates

the heat transfer model with specified boundary conditions. Seciton 3 cross-validates established numerical models with reference to published works. After validating the simulation approach, Section 4 compares four prototypes of compositive PV vacuum glazing and Section 5 gives a detailed analysis of the influence from critical design factors, contributing to an instructive guidance for the design optimization of compositive PV vacuum glazing. There are several important areas to which this study makes an original contribution: (1) An air cavity is combined with PV vacuum glazing to further decrease the overall heat transfer coefficient and its specific impact on the glazing thermal performance is quantified; (2) A three-dimensional heat transfer model is established to characterize the temperature and heat flux of four configurations of PV-VG, which are derived from combinations of the PV location (facing indoor/outdoor environment) and the existence (with/without) of the air cavity between PV and vacuum glazing; (3) A comprehensive sensitivity analysis is conducted for the thermal performance of PV-VG based on key design parameters, including the thermal property of components, dimension and distribution of vacuum pillars, configuration of Low-E coatings and width of air cavity; (4) A guideline is provided for the initial design of PV-VG to enhance the thermal performances of Low-Energy buildings.

2 Methodology

COMSOL Multiphysics, a powerful software tool based on finite element method, is chosen to simulate the complex heat transfer process of compositive PV vacuum glazing. This platform has been used to conduct PV system related research with a demonstrated modelling accuracy [26–28]. Thermal models were built in COMSOL Multiphysics 5.4 to investigate the difference of using polymer and glass layers behind the solar cell [26]. The model was validated by experiments and the temperature distribution showed good agreement. The same tool was used by Jha and Tripathy to describe the thermal behavior of the PV panel and the finite element model showed higher accuracy in temperature predictions than the nominal operating cell temperature model [27]. Therefore, a 3D model is established on the COMSOL Multiphysics platform to represent the compositive structure and simulate the heat transfer by coupling physical interfaces of the heat transfer in solids and surface to surface radiation. The former involves thermal conduction, convection as well as radiation between a certain surface and the ambiance, while the latter mainly deals with radiative heat exchange between surfaces.

2.1 Heat transfer analysis

For a PV vacuum glazing containing four layers of glass without an air layer, the laminated

PV glazing and vacuum glazing units are simply combined using polyvinyl butyral [8]. Vacuum glazing is generally separately prepared and the solar cell is then encapsulated to fabricated the PV vacuum glazing with three glass layers [16]. Due to the complex structure of PV-VG, it is difficult to precisely evaluate its thermal performance as many factors need rigorous definitions. Four configurations of PV-VG are investigated in this study as shown in Fig. 1. PVVG is the one with three layers of glass in which PV is facing the outdoor environment while VPVG is also a three-layer structure only with PV facing the indoor environment. The difference between PVVDG and VPVDG also lies in the location of PV, but they include an air cavity between PV and vacuum glazing compared to the former two configurations. Based on the experience from studies on the photovoltaic double glazing, the air cavity should be able to decrease the U-value of PV-VG. PV vacuum glazing integrated with an air cavity and its influence over the overall glazing thermal performance have not yet been explored by existing research studies to the best knowledge of the authors. Therefore, the thermal performance of the proposed four PV-VG configurations will be compared to determine the optimal structure for applications in Low-Energy buildings. Taking PVVG as an example shown in Fig. 1 (a), the complex heat transfer process can be divided into five parts:

1) The front glass sheet: the conductive heat transfer through the glass sheet, convective heat transfer between the ambient air and external surface, short-wave radiation (solar radiation) and long-wave radiation between the external surface and ambiance;

2) The layer of the solar cell and EVA: the conductive heat transfer through the solar cell and EVA;

3) The middle glass sheet: the conductive heat transfer, radiative heat transfer between two inner surfaces of the vacuum gap;

4) The vacuum pillars: the conductive heat transfer through the pillar array;

5) The back glass sheet: the conductive heat transfer, radiative heat transfer between two inner surfaces, convective heat transfer and long-wave radiation between the indoor air and internal surface.

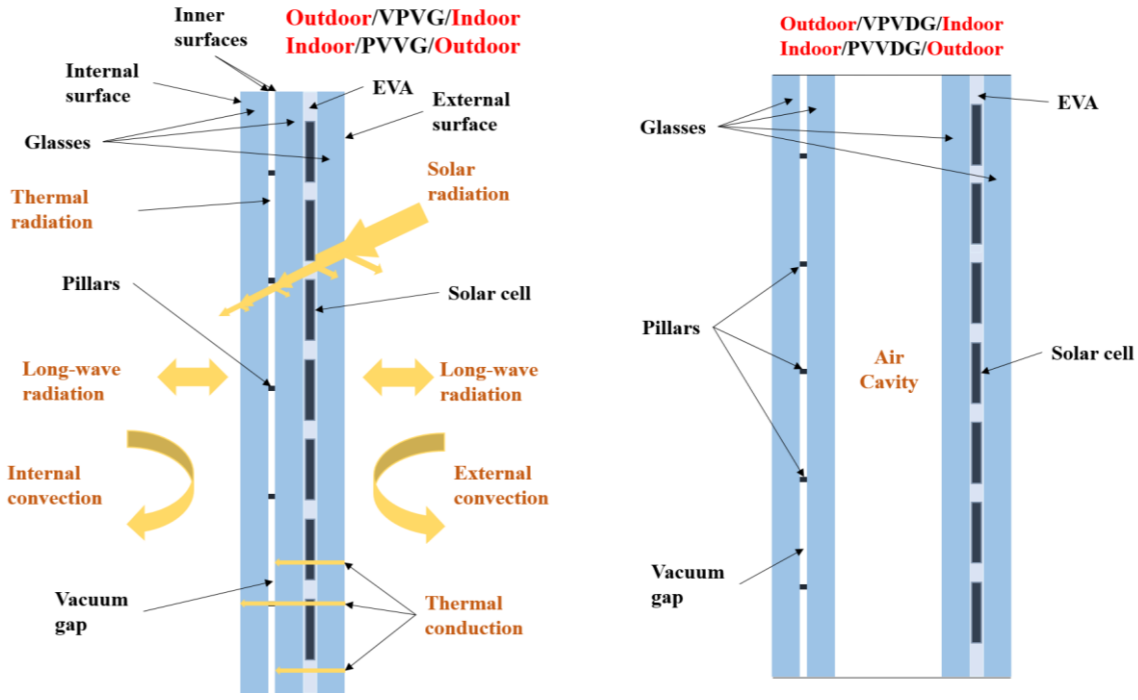

Fig. 1 Different types of PV vacuum glazing and a sample heat transfer illustration

The above illustrative model is set up with the below assumptions:

1) Neglecting the radiative heat transfer between the cylindrical surfaces of the pillar array and two inner glass surfaces;

2) Ignoring the conductive and convective heat transfer of the residual air in the vacuum gap;

3) Assuming only one integral layer to represent solar cells and EVA;

4) Considering merely the central area of the glazing excluding the sealant and frame.

Similar hypotheses can also be found in references [26,29,30]. The gaseous conductive and convective heat transfer is negligible in a vacuum environment of 0.1 Pa or less. From the analysis above, the thermal performance of PV vacuum glazing can be affected by factors including the thermophysical property, dimension of components, separation of vacuum pillars, use of Low-E coatings and PV module design. The effect of these factors is analyzed and discussed in this paper.

2.2 Heat transfer model

The 3D heat transfer models are established in COMSOL Multiphysics based on three general patterns of the heat transfer. The conductive heat flux q_{cond}, convective heat flux q_{conc} and radiative heat flux q_{rad} can be described by Eq. (2)-(4):

$$q_{cond} = -k\nabla T \tag{2}$$

$$q_{conc} = -h_{conv}(T_{ext} - T) \tag{3}$$

$$q_{rad} = -\varepsilon\sigma(T_{amb}^4 - T^4) \tag{4}$$

where k is the thermal conductivity (W/(m·K)); ∇T is the temperature gradient; h_{conv} is the convective heat transfer coefficient (W/(m^2·K)); T_{ext} is the temperature of the external fluid; ε is the surface emissivity; σ is the Stefan-Boltzmann constant; and T_{amb} is the temperature of the ambient environment.

The temperature distribution of different glazing, including the temperature of the internal surface and PV module, can then be predicted by heat transfer models. Furthermore, the overall heat transfer coefficient (U-value) is evaluated by Eq. (5-6) with the acquired temperature distribution and heat flux according to the standard ISO 15099 [31]. U-values have been presented as important indicators for evaluating the thermal performance of PV glazing and vacuum glazing [32,33].

$$U = \frac{1}{1/h_{in} + R_{glazing} + 1/h_{out}} = \frac{Q_{int}}{T_{in} - T_{out}} \tag{5}$$

$$Q_{int} = A(q_{conv} + q_{rad}) \tag{6}$$

where h_{in} is the interior surface heat transfer coefficient, h_{out} is the exterior surface heat transfer coefficient, $R_{glazing}$ is the thermal resistance of composite glazing layers (including the glass layer, air cavity, and any other embedded layers such the PV layer), Q_{int} is the heat flux transferred from the internal surface to the indoor environment without solar radiation [31]; T_{out} is the outdoor temperature; T_{ind} is the indoor temperature and A is the area of the internal surface of PV vacuum glazing.

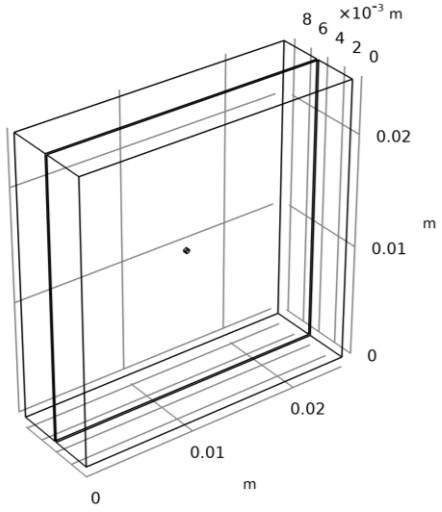

Fig. 2 A simplified 3D geometric model of the vacuum glazing

As the influence from the sealant and frame is out of the scope of this work, the calculated U-value should be the overall heat transfer coefficient of the central window area. To exclude the impact from the glazing edge, a 3D geometric model with only one vacuum pillar is established in Fig. 2 for vacuum glazing. This approach is deemed adequate to predict the thermal responses of vacuum glazing given its symmetric structure, and has been adopted in many existing studies to reduce the computation time [29].

2.3 Boundary conditions

This work aims at describing the thermal response of PV glazing under the steady state, which is as well the experimental condition to determine the overall heat transfer coefficient (U-value) [33,34]. Generally, the guarded hot box calorimeter, used in experiments, is established to keep different temperatures on both sides of the installed target glazing. Experimental approaches for U-values are summed up in [35,36], which also sort the boundary conditions for simulating U-values. It has been mentioned in ISO 15099 [31] that "by definition the thermal transmittance is assumed to be the thermal transmittance without solar radiation". This is also consistent with definitions in many other standards [37–40], as well as the Chinese industry standard JGJ/T 151-2008 by which the prototype glazing is produced [41]. It is also noteworthy that ANSI/NFRC 100-2017 [42] and ASHRAE handbook 2017 agree with such zero solar flux assumptions. In this study, the winter condition settings proposed by ASTM C1199 are adopted to determine window U-values, because the standard clearly specifies surface heat transfer coefficients considering both

the radiative and convective heat transfer [43]. For validation of the simulated U-value, a deviation no more than 0.17 W/(m^2·K) or 10% of the simulated value is acceptable if the U-value is lower than 1.7 W/(m^2·K) or otherwise [42]. Table 1 shows the detailed information of boundary conditions for the heat transfer models in Section 4 and 5. In this study, the heat transfer is modelled in the enclosed hot box environment, so that no solar radiation is involved.

Table 1 Winter condition for the calorimetric hot box to determine the U-value

Winter condition (ASTM C1199)	
Indoor side:	Outdoor side:
$T_{in} = 21℃$	$T_{out} = -18℃$
$h_{in} = 7.7\,W/m^2K \pm 5\%$	$h_{out} = 29\,W/m^2K \pm 10\%$

3 Model validation

The proposed model is validated against extracted data from published articles. The validation involves different glazing types, including vacuum glazing (VG), PV laminated glazing (PVLG), PV double glazing (PVDG) and PV vacuum glazing (PV-VG). The comparisons between heat transfer modelling results and previous publications can demonstrate the accuracy of the proposed method as well as its competence in predicting thermal performances of different windows.

3.1 Validation against vacuum glazing

A guarded hot box was constructed for experimental validation of a finite element model in Ref [34], involving the comparison between a float glass and VG with different sealant widths. Table 2 summarizes the comparison between the testing and modeling results from the above two references and our simulation results with COMSOL Multiphysics 5.4. Judging from the detailed comparison in Table 2, modelling results of Case 1 and 2 show better consistency with those reported in Ref [34]. Modelling results of this study also show a slight increase as validated by the variation of experimental results from Case 1 to Case 2. To further validate the model performance in lower U-values, Case 3 is referenced to a triple vacuum glazing with Low-E coatings investigated using both simulation and experimental methods [44]. In addition, Case 4 makes reference to another research which adopts four layers of Low-E coating to decrease the U-value of triple vacuum glazing to an ideal value of 0.2 W/(m^2·K) [45]. The U-value in Ref [45] is obtained from a mathematical thermal model and validated by a numerical model but not by experiments. In Case 3 and 4, the results from this study have a deviation of 0.08 W/(m^2·K) and

0.09 W/(m^2·K), respectively. The error is acceptable according to ANSI/NFRC 100-2017 [42], by which an error less than 0.17 W/(m^2·K) is considered acceptable when the glazing system has a U-value lower than 1.7 W/(m^2·K). The corresponding model inputs for reference cases are illustrated in Table 3.

Table 2 The comparison between this modelling approach and published works [34]

Reference	Case	Glazing	U-value in references (W/(m^2·K))		U-value in this study (W/(m^2·K))
			Modelling	Experiment	Modelling
[34]	1	VG-1	1.0	0.97±0.08	0.96
	2	VG-2	0.9	1.06±0.09	0.98
[44]	3	TVG-1	0.50	0.53	0.61
[45]	4	TVG-2	0.2	-	0.29

Table 3 Model input according to Reference [34,44,45]

Parameters	Unit	VG-1	VG-2	TVG-1	TVG-2
T_{in}	℃	27.6	37.1	18.2	20
$h_{in,conv}$	W/(m^2·K)	3.31	3.22	6.59	7.7
T_{out}	℃	5.5	12.4	-0.3	0
$h_{out,conv}$	W/(m^2·K)	6.02	4.71	14.94	25
t_g	mm	4	4	4	4
ε	-	0.16, 0.16	0.16, 0.16	0.18, 0.18, 0.84, 0.18	0.03, 0.03, 0.03, 0.03
s_p	mm	25	25	25	30
d	mm	0.4	0.4	0.3	0.3
H	mm	2	2	0.12	0.12

Apart from the U-value, the measured surface temperature of tested samples was also presented in Ref [34], which is listed in Table 4 together with the modeling results in this study. It is found that the developed heat transfer model can accurately predict the glazing surface temperature. The maximum difference between experimental and modelling results is 1.27℃, leading to a relative error of 3.8%. As a result, the developed heat transfer model is successfully cross-validated with a high reliability in predicting the temperature distribution and U-value.

Table 4 The comparison of temperature from Reference [34] and simulation results in this study

Reference	Case	Glazing	External Surface Temperature		Internal Surface Temperature	
			Experiment	Simulation	Experiment	Simulation
[34]	1	VG-1	24.2℃	25.1℃	7.6℃	7.6℃
	2	VG-2	33.1℃	34.4℃	15.5℃	15.0℃

3.2 Validation against existing PV glazing and PV vacuum glazing

Compared with the structure of PVLG, PVDG has a 12 mm air cavity and one more glass sheet with varied thicknesses of each layer. As for PV-VG, the glass sheet before the PV module is replaced by a vacuum glazing unit. Because only limited parameters are provided in [16,46,47], the environment temperature and heat transfer coefficient given in Table 1 will be utilized in this simulation. Additional model inputs are listed in Table 5.

Table 5 Model inputs for PVLG, PVDG and VPVG in addition to ASTM C1199

Parameters	PVLG	PVDG	PV-VG
ε	0.84, 0.84	0.05, 0.88	0.03, 0.03
$t_g(mm)$	6	4	4
$k_g(W/mK)$	0.76	1	1

Table 6 summarizes the validation results with Case 5 to Case 7. For Case 5 and 6, it is found that the modeling results of PVLG and PVDG in this study are closer to values in existing references [46,47]. The thermal transmittance of PVDG is lower than that of PVLG owing to the air cavity, which contributes to a less heat transfer with lower thermal conductance. As for Case 7 (i.e. PV-VG), good agreement is also achieved between experimental and simulation results. The simulated U-value is obtained from the condition that both inner surfaces in the vacuum gap are coated with a Low-E coating ($\varepsilon = 0.03$).

Table 6 The comparison between simulative approach and published work [16,46,47]

Reference	Case	Glazing	U-value (W/(m^2·K)) in references	U-value (W/(m^2·K)) in this study
[47]	5	PVLG	5.18	5.00

[46]	6	PVDG	2.64	2.55
[16]	7	PV-VG	0.8	0.84

Based on the comprehensive comparisons with previous works, the proposed method can achieve adequate accuracy in predicting the temperature distribution and U-value for different glazing configurations. The reliable heat transfer model can then be used to compare different composite PV vacuum glazing and investigate the potential influence of various design factors.

4 Thermal performance modeling

According to the winter condition specified in ASTM C1199, this section compares the thermal performance of existing VPVG (Fig. 3(a)) and proposed hybrid VPVG integrated by an air cavity (i.e. VPVDG shown in Fig. 3(c)). VPVDG has the same setting as VPVG except that the 12 mm wide cavity is filled with air with an extra glass layer. Only the two surfaces facing the vacuum gap are coated ($\varepsilon = 0.03$). Section 3.2 has discussed one configuration of VPVG whose vacuum gap faces the outdoor environment (i.e. cold side). This section also discusses their inversed configuration: PVVG (Fig. 3(b)) and PVVDG (Fig. 3(d)), where the PV module is placed in front of the vacuum gap and faces the outdoor environment. Table 7 summarizes detailed input parameters of PV-VGs.

Table 7 Input parameters of PV-VG

Parameters	Values
Stainless-steel pillar thermal conductivity	20 W/(m·K)
Pillar diameter	0.4 mm
Pillar height	0.2 mm
Pillar separation	25 mm
Glass thermal conductivity	1 W/(m·K)
Glass thickness	4 mm
Silicon solar cell thermal conductivity	148 W/(m·K)
PV layer thickness	2 mm
Low-E coatings	0.03, 0.03

Four models are established to compare the temperature of the “PV layer” and U-value of whole composite glazing. The geometric models of these glazing units are illustrated in Fig. 3,

which highlighted the coated surfaces in circles as Surface 1 and 2 in Fig. 3(a), (b), (c) and Surface 3 and 4 in Fig. 3(d). Free triangular elements are used for the mesh generation and the mesh size for vacuum pillars is smaller than the remaining geometry. As shown in Table 8, the surface temperature of VPVG only changes a bit when the mesh size becomes finer. Thus, the combination of "normal" and "fine" will be used for grid generation to save the computational time. Fig. 4 shows details of the generated grid, where the bottom of the vacuum pillar with a radius of 0.2 mm is divided into eight small triangles (See Fig. 4 (b)).

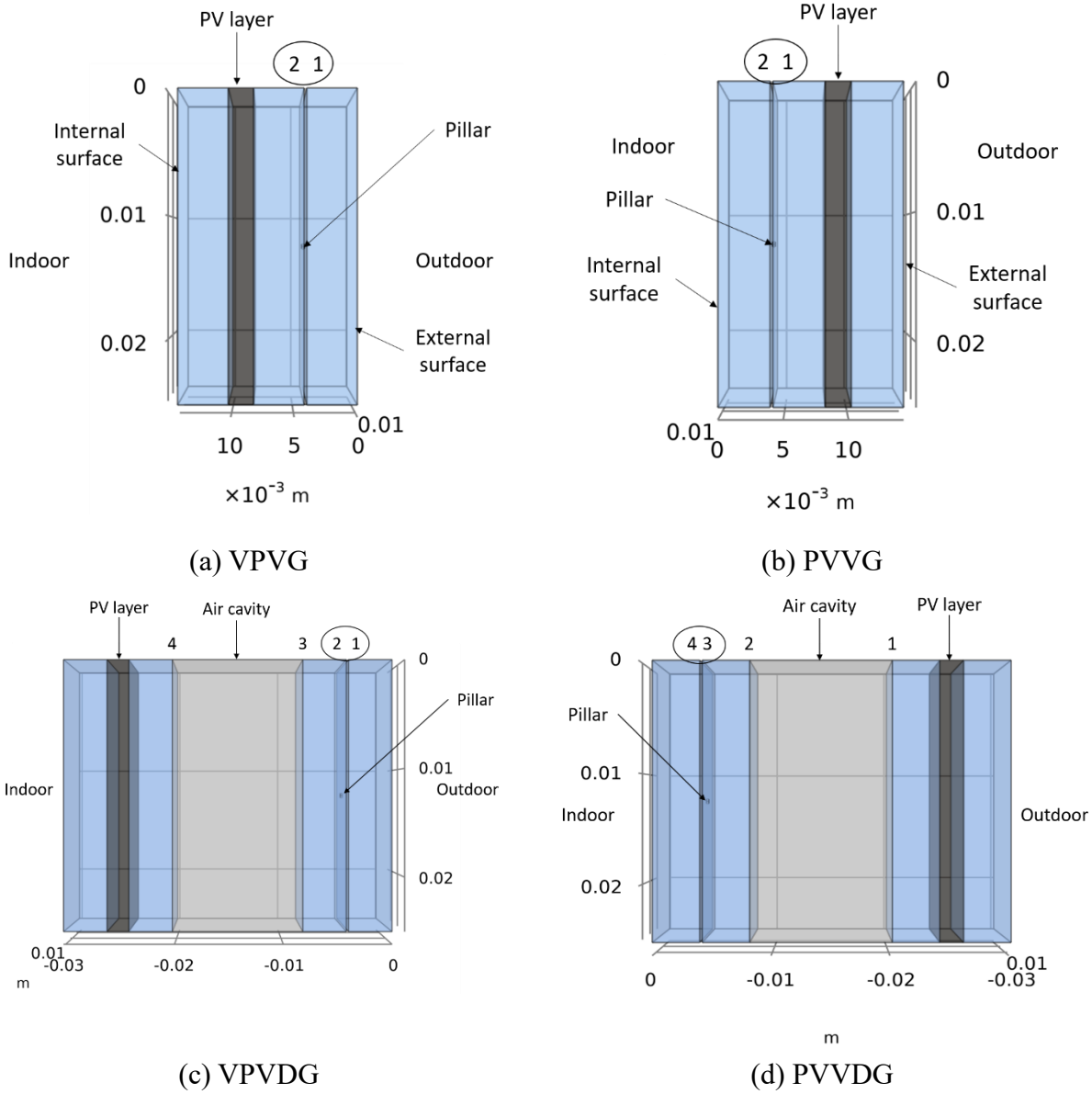

Fig. 3 The geometry models with one vacuum pillar in the center

Table 8 Grid settings and independence test results for VPVG

General mesh size	Pillar mesh size	Internal surface temperature (℃)	External surface temperature (℃)
Normal	Fine	17.0	-16.7
Fine	Fine	17.0	-16.7
Fine	Finer	16.9	-16.7

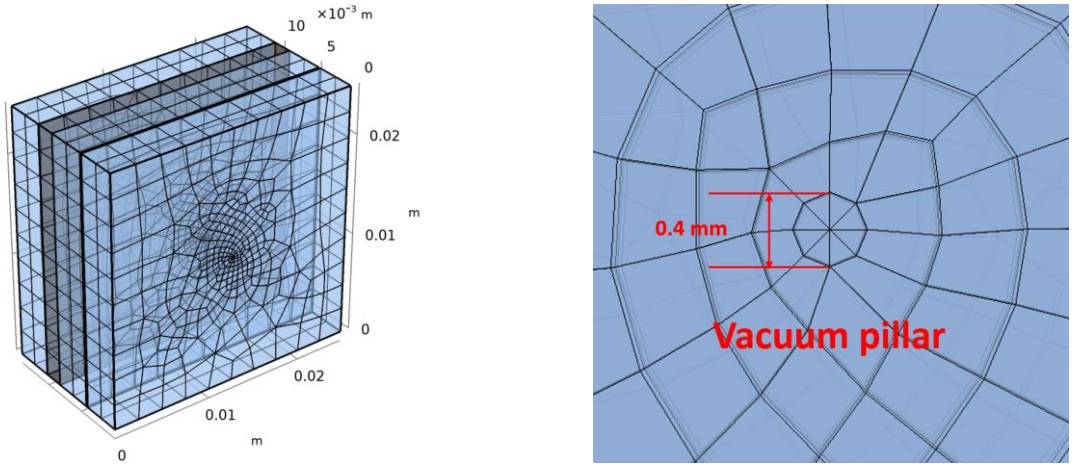

(a) (b)

Fig. 4 Geometric grid for VPVG: (a) the whole structure; (b) details of the vacuum pillar

4.1 VPVG and PVVG modeling results

Fig. 5 (a) shows the temperature distribution of the whole structure of VPVG under the winter condition (i.e. no solar radiation). Apparently, the front glass sheet has the lowest temperature (-16.9 ℃) when facing the cold outdoor environment. For the inner surface in the vacuum gap, it can be clearly seen in Fig. 5 (b) that the temperature around the vacuum pillar is lower than other areas given its direct contact with the colder outside glass panel of VG (i.e. the cold bridge effect). Under this circumstance, the PV module temperature (16.6 ℃) is much higher than that of the vacuum pillar (0.2 ℃). The temperature difference between the external and internal surface is 33.6 ℃, indicating an outstanding thermal insulation performance. The internal surface temperature can be kept at 16.8 ℃ while the outdoor environment only has a temperature of -17.8 ℃. The U-value of VPVG is thus as low as 0.84 W/(m^2·K).

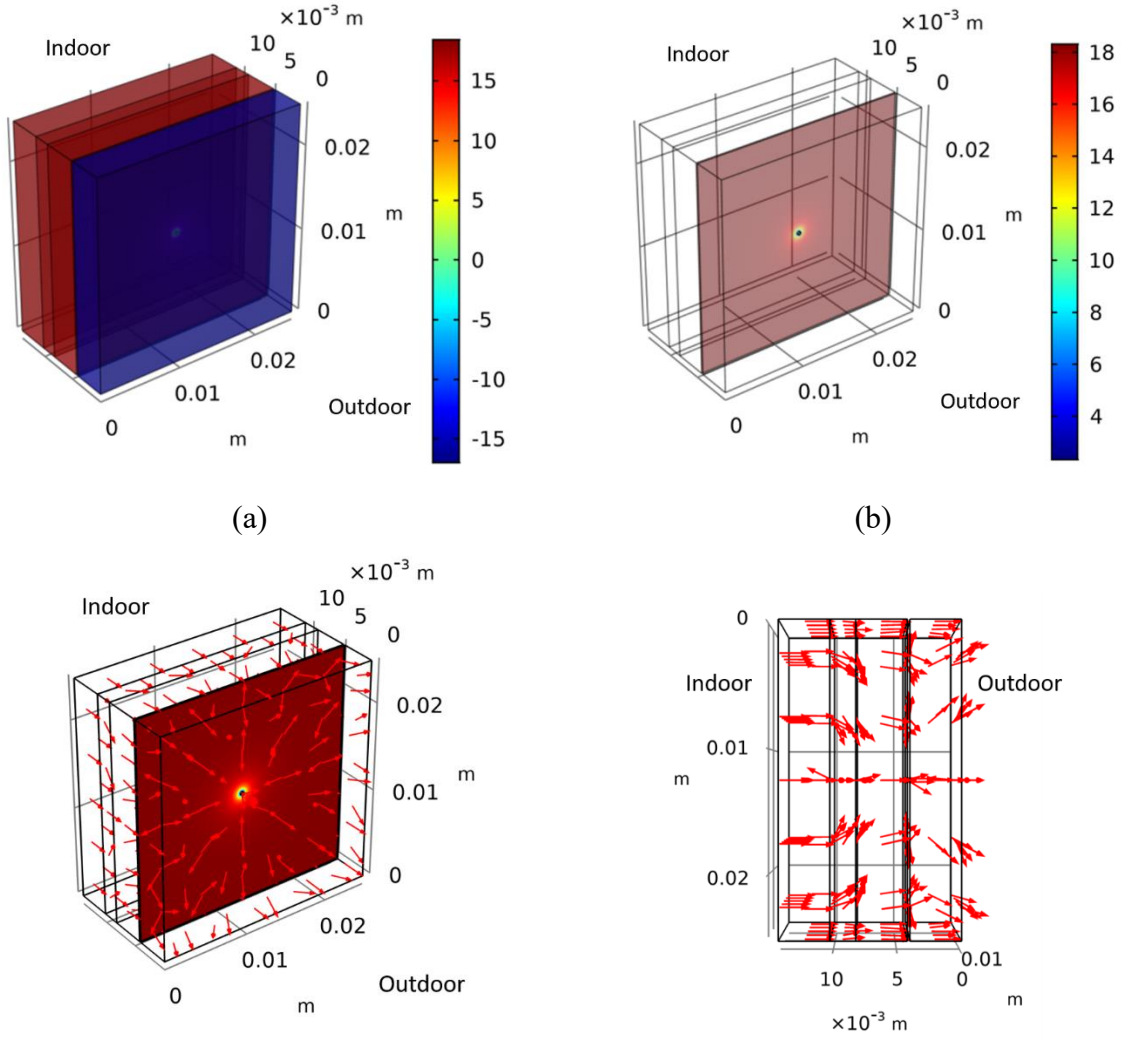

Fig. 5 Temperature distribution and heat flow direction of VPVG

The arrows in Fig. 5 (c) and (d) illustrate the direction of heat flow passing through the whole structure of VPVG. The heat flow starts from the innermost glass facing the indoor environment and is conducted to the middle glass sheet, where the arrows gradually concentrate towards the central vacuum pillar and then spread out in the last glass sheet.

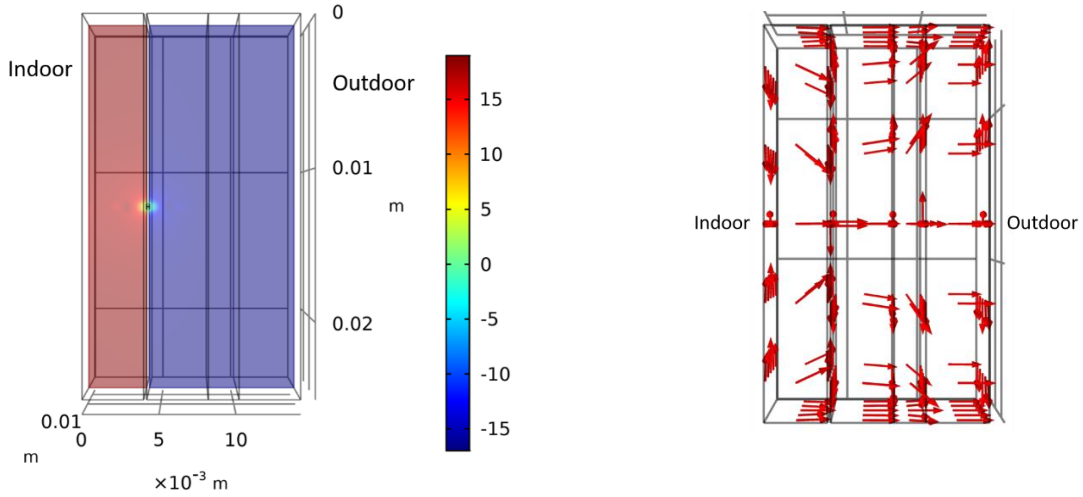

(a) (b)

Fig. 6 Temperature distribution and heat flow direction of PVVG

Regarding PVVG, the temperature distribution is reversed as the PV module is facing the cold side. As shown in Fig. 6(a), the temperature around the vacuum pillar is -0.2 ℃, much higher than the temperature of the PV module (-16.7 ℃). The arrows in Fig. 6(b) also show a similar heat flow pattern which concentrates on the vacuum pillar at first but starts spreading in the vacuum glazing part. The U-value of PVVG under the winter condition is also 0.84 W/(m^2·K), the same as VPVG, which echoes with the result from the reference [16]. Compared with VPVG, the PV module temperature is much lower in PVVG and can therefore help alleviate the decline of its conversion efficiency. In addition, placing the PV module in front of vacuum glazing can harvest more solar radiation. Given the above reasons, PVVG is more suitable for applications in the cold climate than VPVG, which is consistent with a previous climate applicability study [13] .

4.2 VPVDG and PVVDG modelling results

The main difference between VPVDG and VPVG is the air cavity located between vacuum glazing and PV glazing, just as the situation between PVVDG and PVVG. A study emphasized that the convective heat transfer would become comparable if the air gap width exceeded 15 mm in double glazing [48], otherwise the conduction dominates other patterns of the heat transfer. As the air cavity width is only 12 mm, it is assumed that the air is not circulating in the air-tight cavity under the steady state and the influence of convection is ignored in this study. Thus, the heat is transferred within the cavity mainly by two patterns, i.e. conduction through the air and radiation between inner surfaces. Fig. 7 shows the temperature distribution and heat flow direction of

VPVDG and PVVDG. Similar temperature distributions can be found between VPVG and VPVDG as well as between PVVG and PVVDG. It can be distinguished by the arrows that the heat flow at the front glass differs with the reversed configurations of PVG and VG.

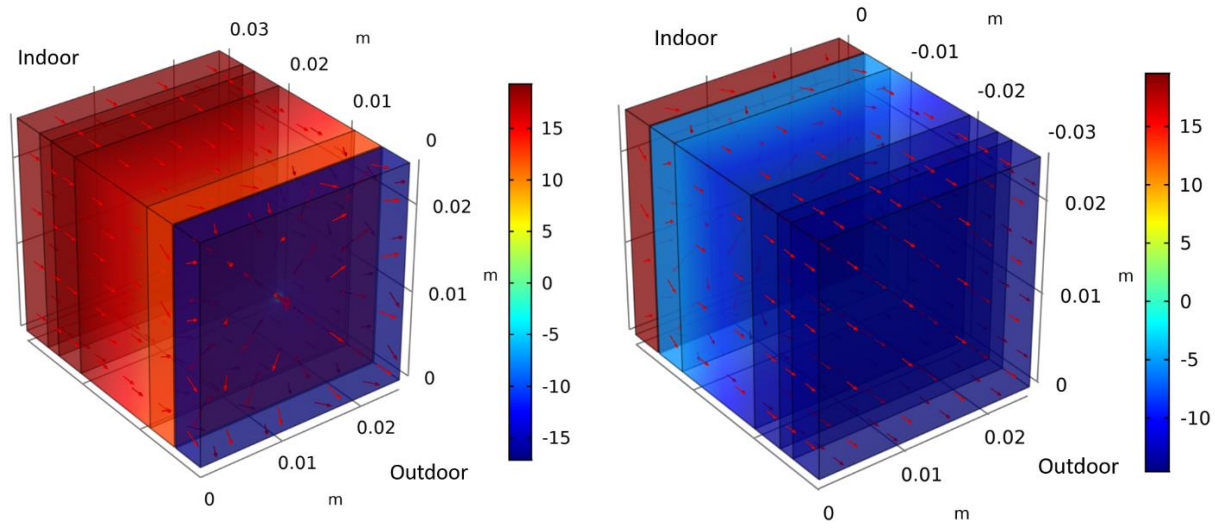

(a) VPVDG (b) PVVDG

Fig. 7 Temperature distribution and heat flow direction of VPVDG and PVVDG

Since the air acts as a thermal insulation medium, the PV module has a higher temperature (17.6 ℃) in VPVDG compared with that of VPVG due to less heat loss. Although a higher temperature may impair the efficiency of power generation, the small temperature difference of 1.0 ℃ may almost be ignored. Considering the difference of U-values shown in Table 9, VPVDG should be preferred over VPVG. As for the comparison between the other two configurations, the PV module temperature of PVVDG (-17.1 ℃) is slightly lower than that of PVVG. What is more, the U-value of PVVDG (0.63 W/(m^2·K)) turns out to be the lowest, indicating the best thermal performance achieved by this structure. The additional air cavity with a width of 12 mm helps to decrease the U-value from 0.84 W/(m^2·K) to 0.65 W/(m^2·K) for VPVG and VPVDG, and from 0.84 W/(m^2·K) to 0.63 W/(m^2·K) for PVVG and PVVDG. The performance improvement is up to 23.0% and 25.1%. Moreover, the PV conversion efficiency of PVVG and PVPDG can be guaranteed as long as it is facing the cold outside environment with more available solar radiation compared with that of VPVG and VPVDG.

Table 9 Average temperature and U-value of different glazing

Glazing	Internal surface	External Surface	PV module	U-value

	Temperature (℃)	Temperature (℃)	Temperature (℃)	(W/(m^2·K))
VPVG	16.8	-16.9	16.6	0.84
VPVDG	17.7	-17.1	17.6	0.65
PVVG	16.8	-16.9	-16.7	0.84
PVVDG	17.8	-17.2	-17.1	0.63

5 Impact of critical design factors

In addition to the thermophysical properties of different composite glazing and components, the influence of critical design factors on the thermal performance is subject to detailed analyses across the previous four glazing configurations. The overall heat transfer coefficient (i.e. the U-value) is evaluated as the thermal performance indicator in this session. The concerning factors and corresponding components are listed in Table 10, while heat transfer models comply with boundary conditions in Table 1. The parameter variation range in Table 10 is mainly sourced from the data in exiting literature [3,11] and WINDOW 7.6 [49], and used to quantitatively analyze the impact on the U-value. The following models are established assuming both surfaces in the vacuum gap Low-E coated ($\varepsilon = 0.03$), except when investigating the impact of the coating emissivity.

Table 10 Potential factors affecting the U-value

Component	Specification	Range
Glass	Thermal conductivity	0.2-1.2 W/(m·K)
Vacuum pillar	Thermal conductivity	1-40 W/(m·K)
	Separation	20-60 mm
	Diameter	0.3-0.6 mm
	Height	0.1-0.4 mm
Low-E coating	Emissivity	0.013-0.313
Air cavity	Width	3-15mm

5.1 Influence of the glass sheet's thermal property

The glass sheet is the major component for composite windows, in which a lower thermal conductivity can contribute to better thermal performances. According to the glass library built by the Lawrence Berkeley National Laboratory [50], the glass thermal conductivity ranges from 0.14 to 1.38 W/(m·K). The simulated thermal conductivity varies from 0.3 to 1.2 W/(m·K) in this paper

and is therefore within a rational range. Fig. 8 compares the impact of glass thermal conductivity on the thermal performance of four glazing configurations. As shown in Fig. 8, the U-value of all glazing configurations increases linearly with the thermal conductivity of the glass sheet. This tendency is more apparent for VPVG and PVVG with a much higher slope than the other two cases. Among all configurations, VPVDG and PVVDG show a lower sensitivity to the glass thermal conductivity. In terms of the variation ratio, the U-value is decreased by around 64.8%, 59.1%, 64.9% and 58.6% for VPVG, VPVDG, PVVG and PVVDG, respectively. Given the change in regular patterns, the thermal conductivity of glass sheets is suggested to be as low as possible for better thermal insulation.

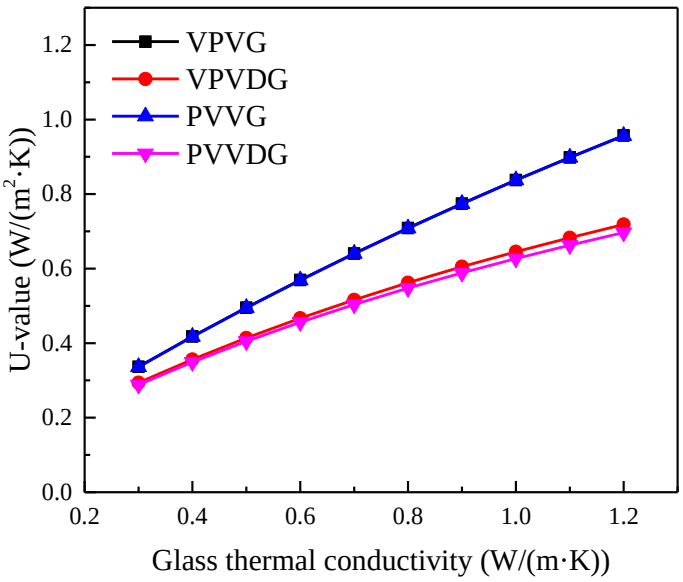

Fig. 8 The effect of glass sheet on the U-value

5.2 Influence of vacuum pillar

The vacuum pillar array is the indispensable part of vacuum glazing to separate and support two glass sheets within a vacuum environment, where conductive and convective heat exchanges can be minimized. In order to maintain a vacuum of 0.1Pa [51], the array requires proper materials and designs to endure the great extrusion force from glass sheets.

As mentioned in the Chinese standard GB/T 38586-2020 [52], the vacuum pillar usually has a diameter of 0.3~0.5 mm, a height of 0.1~0.4 mm, and separation of 20~60 mm. It can also be found in the existing literature [3] that the above distribution ranges are 0.3~0.6 mm, 0.12~0.72 mm, 15~60 mm for stainless-steel pillars. Moreover, the material of the vacuum pillar is normally

stainless-steel, but it can be replaced by the aerogel material with an extraordinary thermal conductivity of 0.032 W/(m·K) as reported in [20]. According to these references, a reasonable distribution range is determined for this study.

The separation, the diameter and height of a single pillar, as well as the material thermal conductivity of the pillar array are examined to quantify their impact on the overall U-value of the composite glazing as per Fig. 9. In Fig. 9(a), the pillar thermal conductivity affects the U-value greatly within the range from 1 to 10 W/(m·K), whereas the effect becomes weak after exceeding this range. The U-value of VPVG and VPVDG increases by merely 0.06 W/(m^2·K) and 0.05 W/(m^2·K) when increasing the pillar thermal conductivity from 11 to 40 W/(m·K), while it can be improved by about 40.7% when decreasing the conductivity from 10 to 1 W/(m·K). It can therefore be concluded that the U-value can be significantly reduced if the stainless-steel pillar is replaced by a proper material with low thermal conductivity and high compression resistance, for instance, aerogel with a thermal conductivity of 0.54 W/(m·K) [52].

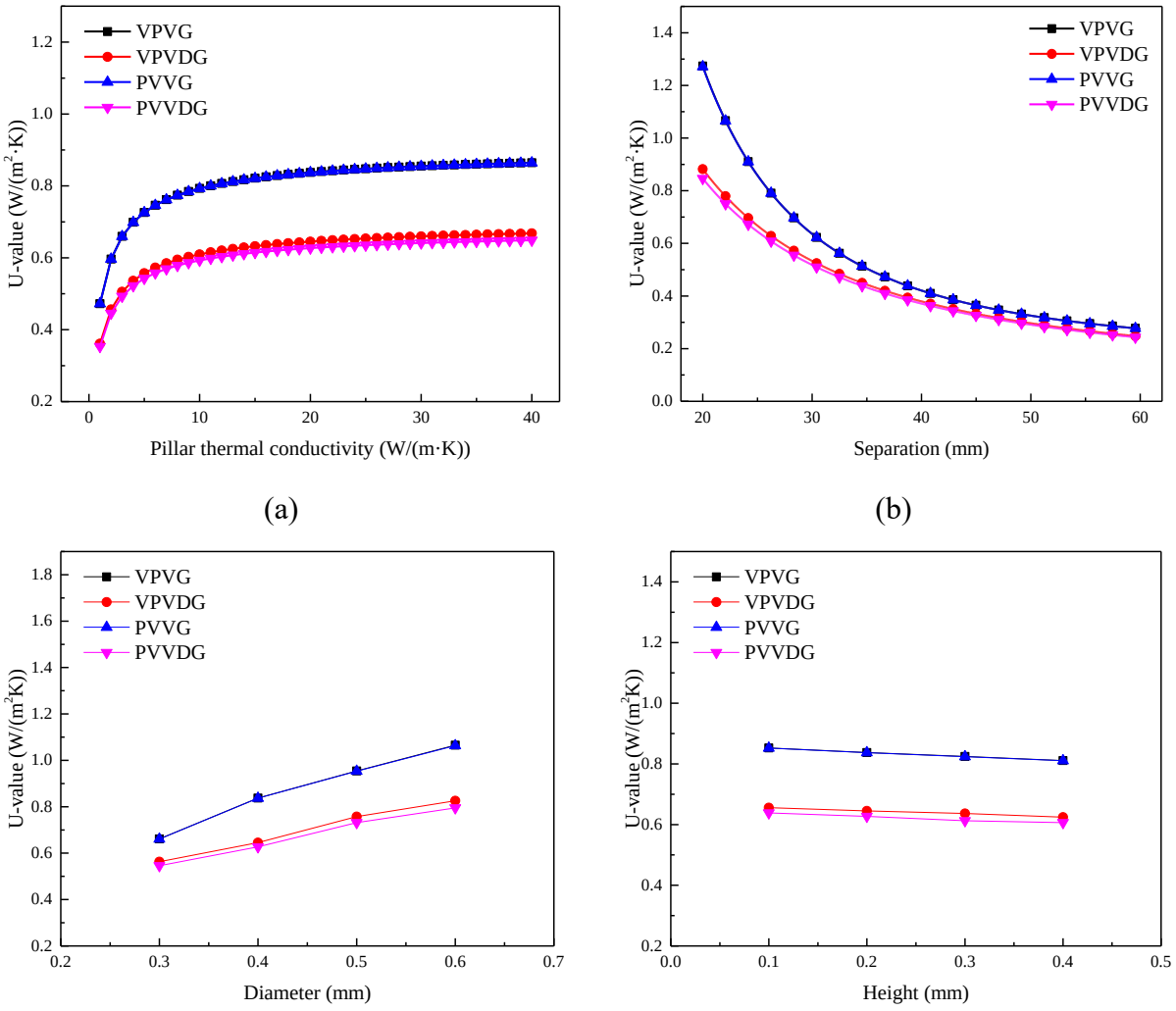

(c) (d)

Fig. 9 The effect of vacuum pillars on the U-value

The relationship between the pillar array density and glazing thermal performance is presented in Fig. 9(b). The U-value generally drops with the separation of pillars while fluctuates slightly when the separation is around 40 mm, echoing with the key findings on VG in existing research where the variation gradually levels off in low pillar densities [53,54]. Therefore, the separation is suggested to be as large as possible as long as the array can endure the compression from glass sheets. A tremendous improvement of the thermal performance can be achieved by enlarging the pillar separation from 20 mm to 60 mm. For instance, the U-value of VPVG can be reduced by 79% from 1.19 to 0.25 W/(m^2·K). Among four glazing configurations, PVVDG with a pillar separation of 60 mm can achieve the lowest U-value of 0.23 W/(m^2·K), which approximates the reported U-value of 0.22 W/(m^2·K) for a triple vacuum glazing [11].

On the contrary, the U-value obviously rises with the diameter of pillars as shown in Fig. 9(c), as larger diameters increase the contact area of the heat exchange between pillars and glass sheets (i.e. enlarged cold/heat bridge effect). The result is similar to that reported in [3], so that a smaller diameter is preferred for the sake of thermal insulation. The reduction of U-values is 37.9%, 31.8%, 37.9% and 31.4% for VPVG, VPVDG, PVVG and PVVDG respectively when decreasing the pillar diameter from 0.6 mm to 0.3 mm.

At last, the variation with pillar heights (i.e. the width of the vacuum gap) is illustrated in Fig. 9(d), which indicates a minor impact on thermal performance. The overall heat transfer coefficient decreases by 0.03 W/(m^2·K) (5.0%) when the height varies from 0.1 mm to 0.4 mm for the case of PVVDG. Other cases also show slight variations between 4.8-4.9%, which is similar to the effect of pillar thermal conductivity within the range of 11-40 W/(m·K).

5.3 Influence of Low-E coatings

Low-E coatings reduce the radiative heat transfer through decreasing the emissivity of standard clear glass (0.84) to the lowest available emissivity (0.013) in the library of Window 7.6 [49]. Therefore, this paper quantifies the impact of Low-E coatings on the composite PV vacuum glazing with the emissivity ranging from 0.013 to 0.313. Different scenarios are designed as: (1) The inner surface close to the indoor ambiance is uncoated while the other inner surface in the vacuum gap is coated; (2) Both inner surfaces in vacuum gap are coated; and (3) Inner surfaces of the air cavity instead of the vacuum gap are coated for PVVDG.

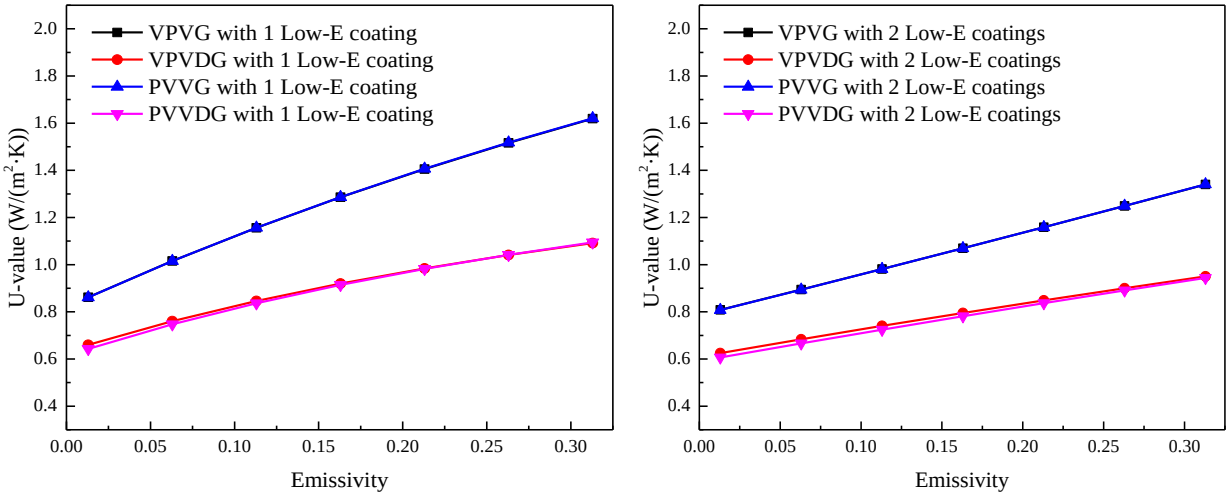

(a) Scenario 1 (b) Scenario 2

Fig. 10 The effect of the Low-E coating on the U-value for Scenario 1 and 2

Fig. 10(a) shows the influence from the Low-E coating in the first scenario. The U-value of VPVG and PVVG tends to be more sensitive to the increase of the emissivity with a variation up to 0.8 W/(m^2·K). In contrast, the U-value of VPVDG and PVVDG only varies by 0.4 W/(m^2·K) due to the additional air cavity. The U-value of different glazing configurations has changed between 39.5% and 46.8% across the emissivity range. Similar tendencies can be seen in the second scenario as per Fig. 10(b), where the U-value increases with the growing emissivity. On condition that the lowest possible emissivity is 0.013 [49], the minimum U-value is merely 0.6 W/(m^2·K) for PVVDG. However, it can be also found that the improvement is not obvious for these cases when adding another layer of Low-E coating. The maximum variation of U-value is only 0.3 W/(m^2·K) across the emissivity range for all four cases, while the rate of change drops with reducing emissivity. The above findings echo with similar research on the effect of a second Low-E coating for PVDG and VG respectively [10,55].

As for Scenario 3, the U-value of PVVDG decreases slowly with the emissivity of Low-E coatings in the air cavity and is clearly different from other scenarios as per Fig 10. The overall heat transfer coefficient stays above 1.1 W/(m^2·K) in Scenario 3, which is higher than the maximum of 0.9 W/(m^2·K) in scenario 2. Coating the inner surfaces in the air cavity is less effective on the overall thermal performance of composite glazing. It can be attributed to the fact that radiation dominates the heat transfer process in the narrow vacuum gap where the coating can block more thermal energy.

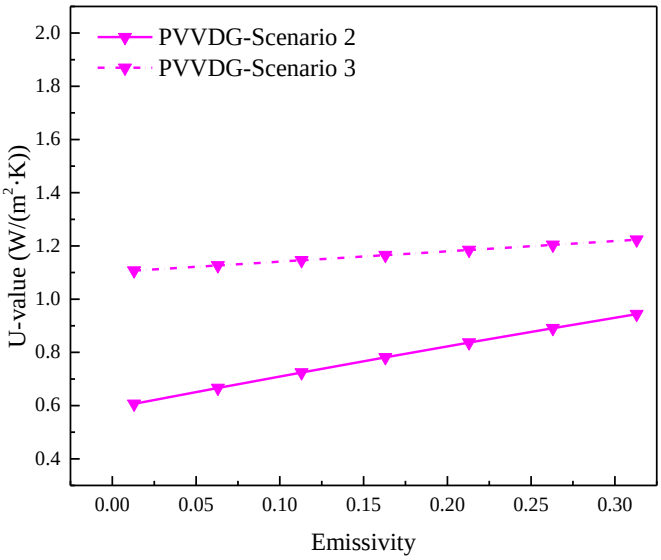

Fig. 11 The effect of the Low-E coating on the U-value for Scenario 2 and 3

5.4 Influence of air cavity

The air cavity contributes to about a 46% reduction in the U-value of PVDG compared with that of PVLD in Section 3.2. When the air cavity is added to vacuum glazing, such reduction can be anticipated to be less conspicuous. Fig. 12 shows the effect of the air cavity width on the U-value of VPVDG and PVVDG. U-values of these two glazing configurations are negatively correlated to the air cavity width, with a reduction of 19.6% for VPVDG and 21.49% for PVVDG across the variation range. The result complies with the variation of the heat transfer coefficient when the air cavity width is less than 15 mm as reported in [56]. Nonetheless, a wider air cavity is suggested to improve the thermal performance as much as possible.

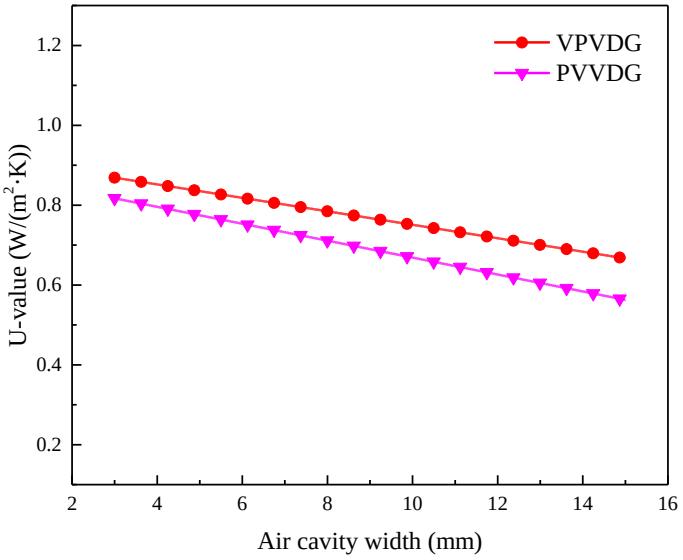

Fig. 12 The effect of the air cavity width on the U-value

5.5 Discussion of impact analysis

This section has investigated the influence from glass sheets, pillars, Low-E coatings and the air cavity on the overall heat transfer coefficient of four glazing configurations. The factors can be divided into two categories according to their impact. The first category consists of the thermal conductivity of glass sheets, diameter and height of vacuum pillars, Low-E coating and the width of the air cavity, to which the U-value correlates linearly. Except for the width of the air cavity and height of vacuum pillars, the U-value shows positive correlations with the first category of factors. In other words, the overall heat transfer coefficient can be decreased by lowering the thermal conductivity of glass sheet, diameter of vacuum pillars and emissivity of Low-E coatings, while increasing the width of vacuum gap and air cavity. The second category includes the thermal conductivity and separation of vacuum pillars, which contribute to the nonlinear response of the U-value. Enlarging the separation to the maximum safety allowance and lowering the thermal conductivity of pillars to below 10 W/(m·K) can significantly improve the thermal performance. It is worth mentioning that the pillar array should follow four design constraints [51,54]: (1) the compressive stress on the pillar array should be under the material's compressive stress limit, roughly 1.5 GPa for stainless-steel; (2) 4 MPa is the generally allowable tensile stress for the glass and cannot be exceeded for pillars; (3) conical indentation fractures do not occur; and (4) the thermal conductance of the pillar array is preferably less than 0.4 W/(m·K). Limited by these rules, the pillar array density has a proper range as determined by the height, radius, and thickness of glass. Detailed equations to calculate the compliance with above constraints can be found in [20],

whereas this paper only investigates the impact of separation in a normal range as per existing standards and literature. The optimal thermal performance for all glazing configurations can be determined by considering the negative and positive impact from all design factors. Table 11 further summarizes the maximum variation of the overall heat transfer coefficient (i.e. the sensitivity index) as affected by these design factors. A positive percentage means that the U-value increases with the growing design factor while a negative one indicates that the U-value declines with the growing design factor. The glass thermal conductivity, separation and diameter of vacuum pillars, and emissivity of Low-E coating are identified as high-impact factors as concluded from Table 11. The pillars thermal conductivity below 10 W/(m·K) also has a significant impact. In addition, the rate of change of the U-value depends on the distribution range of design factors in the third category.

Table 11 Summary of the maximum U-value improvement with critical design factors

Factors	Unit	Range	Improvement proportion of U-value				Category
			VPVG	VPVDG	PVVG	PVVDG	
Glass thermal conductivity	W/(m·K)	0.2-1.2	64.8%	59.1%	64.9%	58.6%	1
Pillar thermal conductivity	W/(m·K)	1-10	40.4%	40.8%	40.4%	40.4%	2
Pillar thermal conductivity	W/(m·K)	11-40	7.4%	7.9%	7.4%	7.8%	2
Separation	mm	20-60	-79.0%	-72.7%	-79.1%	-72.1%	2
Diameter	mm	0.3-0.6	37.9%	31.8%	37.9%	31.4%	1
Height	mm	0.1-0.4	-4.9%	-4.8%	-4.9%	-5.0%	1
Emissivity (single coating)	-	0.013-0.313	46.8%	39.5%	46.8%	41.3%	1
Emissivity (double coatings)	-	0.013-0.313	39.7%	34.2%	39.7%	35.7%	1
Air cavity width	mm	3-15	-	-19.6%	-	-21.5%	1

6 Conclusions

PV vacuum glazing is a multifunctional building envelope design that can generate renewable power and serve thermal insulation and daylight control purposes. Research related to different

configurations of PV vacuum glazing is still rare to date, let alone the innovative structure integrated by an intermediate air cavity. This paper presents a robust modelling approach with COMSOL Multiphysics to investigate the thermal properties of different composite glazing integrated by the vacuum layer, photovoltaic module, and air cavity. The complex theoretical heat transfer process is explored, and a numerical model is built based on reasonable assumptions for the standard winter condition. The modelling approach is then cross-validated with published heat transfer simulations and experimental data on the temperature distribution and U-value for vacuum glazing, photovoltaic laminated glazing and double glazing as well as vacuum photovoltaic glazing. The validated model is then used to compare the thermal performance of the vacuum photovoltaic glazing, photovoltaic vacuum glazing as well as proposed vacuum photovoltaic double glazing and photovoltaic vacuum double glazing. Impact analyses of key design factors are also conducted to guide the optimal design of compositive photovoltaic vacuum glazing for improving thermal performances. Some important conclusions are listed below:

1) The three-dimensional thermal modeling by COMSOL Multiphysics is reliable in determining the temperature distribution as well as the overall heat transfer coefficient. A small average relative error of 2.4% is achieved for VG, PVLG, PVDG and PV-VG.

2) Compared with configurations without the air cavity (i.e. VPVG and PVVG), the U-value can be reduced by 19.6% for the case of VPVDG and 21.5% for PVVDG. PVVDG can achieve superior thermal and potential power performances as it has the lowest U-value and PV module temperature.

3) The glass thermal conductivity, separation and diameter of vacuum pillars and emissivity of Low-E coatings are identified as dominant influencing factors on the glazing thermal performance. In contrast, the pillar thermal conductivity beyond 10 W/(m·K) and width of vacuum gap only have relatively weak impacts.

4) The overall heat transfer coefficient can be decreased by lowering the thermal conductivity of glass sheets and pillars, diameter and density of vacuum pillars and emissivity of Low-E coatings, while increasing the width of the vacuum gap and air cavity. The lowest U-value can be achieved as 0.23 W/(m^2·K) in PVVDG with a pillar separation of 60 mm, and the thermal performance can be further improved with a global optimization.

5) One layer of Low-E coating can play a significant role in reducing the radiative heat transfer and the corresponding U-value, whereas the second layer brings a limited improvement and is therefore not cost-effective.

6) This research provides a guide for the selection of different composite PV vacuum glazing configurations for optimized thermal performances. It can also be used as references for further design improvements of the proposed glazing configuration and promote its integration with whole building simulations. Such novel glazing systems can also facilitate the expansion of renewable applications and corresponding sustainable building designs and retrofitting.

This research focuses on the heat transfer modelling and calibrations for composite PV vacuum glazing under the winter condition, in which the influence of solar radiation is not considered. Future works will thoroughly explore the coupled dynamic power and thermal performance of such composite PV vacuum glazing in real-time weather. The width of the air cavity within VPVDG and PVVDG is recommended to be enlarged for lower U-value. However, convective heat transfer will become dominant and not negligible when the width goes beyond 15 mm, requiring further discussions in future works. Detailed global sensitivity analyses and optimizations will also be conducted to obtain a feasible final design solution with the consideration of mechanical constraints.

Acknowledgements

This project is supported by the Teaching Postgraduate Studentship Scheme (TPS) of The Hong Kong Polytechnic University and the funding of Research and Integrated Demonstration on Suitable Technology of Net Zero Energy Building (2019YFE0100300).

References

[1] E. Cuce, S.B. Riffat, A state-of-the-art review on innovative glazing technologies, Renewable and Sustainable Energy Reviews. 41 (2015) 695–714. https://doi.org/10.1016/j.rser.2014.08.084.

[2] P.C. Eames, Vacuum glazing: Current performance and future prospects, Vacuum. 82 (2008) 717–722. https://doi.org/10.1016/j.vacuum.2007.10.017.

[3] Y. Fang, T.J. Hyde, F. Arya, N. Hewitt, P.C. Eames, B. Norton, S. Miller, Indium alloy-sealed vacuum glazing development and context, Renewable and Sustainable Energy Reviews. 37 (2014) 480–501. https://doi.org/10.1016/j.rser.2014.05.029.

[4] D. Liu, Y. Sun, R. Wilson, Y. Wu, Comprehensive evaluation of window-integrated semi-transparent PV for building daylight performance, Renewable Energy. 145 (2020) 1399–1411. https://doi.org/10.1016/j.renene.2019.04.167.

[5] W. Zhang, L. Lu, Overall energy assessment of semi-transparent photovoltaic insulated glass units for building integration under different climate conditions, Renewable Energy. 134 (2019) 818–827. https://doi.org/10.1016/j.renene.2018.11.043.
[6] L. Lu, K.M. Law, Overall energy performance of semi-transparent single-glazed photovoltaic (PV) window for a typical office in Hong Kong, Renewable Energy. 49 (2013) 250–254. https://doi.org/10.1016/j.renene.2012.01.021.
[7] N. Skandalos, D. Karamanis, PV glazing technologies, Renewable and Sustainable Energy Reviews. 49 (2015) 306–322. https://doi.org/10.1016/j.rser.2015.04.145.
[8] W. Zhang, L. Lu, X. Chen, Performance Evaluation of Vacuum Photovoltaic Insulated Glass Unit, Energy Procedia. 105 (2017) 322–326. https://doi.org/10.1016/j.egypro.2017.03.321.
[9] J. Peng, Simulation studies on advanced window technologies, Building Simulation. 12 (2019). https://doi.org/10.1007/s12273-019-0517-5.
[10] J. Han, L. Lu, H. Yang, Numerical evaluation of the mixed convective heat transfer in a double-pane window integrated with see-through a-Si PV cells with low-e coatings, Applied Energy. 87 (2010) 3431–3437. https://doi.org/10.1016/j.apenergy.2010.05.025.
[11] E. Cuce, P.M. Cuce, Vacuum glazing for highly insulating windows: Recent developments and future prospects, Renewable and Sustainable Energy Reviews. 54 (2016) 1345–1357. https://doi.org/10.1016/j.rser.2015.10.134.
[12] C. Qiu, H. Yang, W. Zhang, Investigation on the energy performance of a novel semi-transparent BIPV system integrated with vacuum glazing, Building Simulation. (2018) 1–11. https://doi.org/10.1007/s12273-018-0464-6.
[13] J. Huang, X. Chen, H. Yang, W. Zhang, Numerical investigation of a novel vacuum photovoltaic curtain wall and integrated optimization of photovoltaic envelope systems, Applied Energy. 229 (2018) 1048–1060. https://doi.org/10.1016/j.apenergy.2018.08.095.
[14] C. Qiu, Y.K. Yi, M. Wang, H. Yang, Coupling an artificial neuron network daylighting model and building energy simulation for vacuum photovoltaic glazing, Applied Energy. 263 (2020) 114624. https://doi.org/10.1016/j.apenergy.2020.114624.
[15] C. Qiu, H. Yang, Daylighting and overall energy performance of a novel semi-transparent photovoltaic vacuum glazing in di ff erent climate zones, Applied Energy. 276 (2020) 115414. https://doi.org/10.1016/j.apenergy.2020.115414.
[16] A. Ghosh, S. Sundaram, T.K. Mallick, Investigation of thermal and electrical performances of a combined semi-transparent PV-vacuum glazing, Applied Energy. 228 (2018) 1591–1600. https://doi.org/10.1016/j.apenergy.2018.07.040.

[17] A. Ghosh, N. Sarmah, S. Sundaram, T.K. Mallick, Numerical studies of thermal comfort for semi-transparent building integrated photovoltaic (BIPV)-vacuum glazing system, Solar Energy. 190 (2019) 608–616. https://doi.org/10.1016/j.solener.2019.08.049.
[18] A. Ghosh, S. Sundaram, T.K. Mallick, Colour properties and glazing factors evaluation of multicrystalline based semi-transparent Photovoltaic-vacuum glazing for BIPV application, Renewable Energy. 131 (2019) 730–736. https://doi.org/10.1016/j.renene.2018.07.088.
[19] H. Jarimi, K. Qu, S. Zhang, Q. Lv, D. Cooper, Y. Su, S. Riffat, Performance Analysis of an integrated Semi-Transparent Thin Film PV Vacuum Insulated Glazing, Hittite Journal of Science & Engineering. 6 (2019) 275–286. https://doi.org/10.17350/hjse19030000158.
[20] H. Jarimi, Q. Lv, R. Omar, S. Zhang, S. Riffat, Design, mathematical modelling and experimental investigation of vacuum insulated semi-transparent thin-film photovoltaic (PV) glazing, Journal of Building Engineering. 31 (2020) 101430. https://doi.org/10.1016/j.jobe.2020.101430.
[21] K.E.E. Park, G.H.H. Kang, H.I.I. Kim, G.J.J. Yu, J.T.T. Kim, Analysis of thermal and electrical performance of semi-transparent photovoltaic (PV) module, Energy. 35 (2010) 2681–2687. https://doi.org/10.1016/j.energy.2009.07.019.
[22] E. Skoplaki, J.A. Palyvos, On the temperature dependence of photovoltaic module electrical performance: A review of efficiency/power correlations, Solar Energy. 83 (2009) 614–624. https://doi.org/10.1016/j.solener.2008.10.008.
[23] L. Sabri, M. Benzirar, Effect of Ambient Conditions on Thermal Properties of Photovoltaic Cells: Crystalline and Amorphous Silicon, International Journal of Innovative Research in Science, Engineering and Technology. 03 (2014) 17815–17821. https://doi.org/10.15680/ijirset.2014.0312010.
[24] P. Lyons, D. Arasteh, C. Huizenga, Window Performance for Human Thermal Comfort, n.d.
[25] COMSOL Multiphysics, (n.d.). https://www.comsol.asia/.
[26] Y. Du, W. Tao, Y. Liu, J. Jiang, H. Huang, Heat transfer modeling and temperature experiments of crystalline silicon photovoltaic modules, Solar Energy. 146 (2017) 257–263. https://doi.org/10.1016/j.solener.2017.02.049.
[27] A. Jha, P.P. Tripathy, Heat transfer modeling and performance evaluation of photovoltaic system in different seasonal and climatic conditions, Renewable Energy. 135 (2019) 856–865. https://doi.org/10.1016/j.renene.2018.12.032.
[28] H. Fayaz, N.A. Rahim, M. Hasanuzzaman, R. Nasrin, A. Rivai, Numerical and

experimental investigation of the effect of operating conditions on performance of PVT and PVT-PCM, Renewable Energy. 143 (2019) 827–841. https://doi.org/10.1016/j.renene.2019.05.041.

[29] Y. Fang, T.J. Hyde, N. Hewitt, A Novel Building Component Hybrid Vacuum Glazing—A Modelling And Experimental Validation, ASHRAE Transactions. 119(2) (2013) 430–441.

[30] Z. Han, Y. Bao, W. Wu, Z. Liu, X. Liu, Y. Tian, Evaluation of thermal performance for vacuum glazing by using three-dimensional finite element model, 2012. https://doi.org/10.4028/www.scientific.net/KEM.492.328.

[31] ISO, 15099: Thermal performance of windows, doors and shading devices-Detailed calculations, 2003.

[32] J. Peng, L. Lu, H. Yang, An experimental study of the thermal performance of a novel photovoltaic double-skin facade in Hong Kong, Solar Energy. 97 (2013) 293–304. https://doi.org/10.1016/j.solener.2013.08.031.

[33] A. Ghosh, B. Norton, A. Duffy, Measured thermal & daylight performance of an evacuated glazing using an outdoor test cell, Applied Energy. 177 (2016) 196–203. https://doi.org/10.1016/j.apenergy.2016.05.118.

[34] Y. Fang, P.C. Eames, B. Norton, T.J. Hyde, Experimental validation of a numerical model for heat transfer in vacuum glazing, Solar Energy. 80 (2006) 564–577. https://doi.org/10.1016/j.solener.2005.04.002.

[35] Y. Sun, Y. Wu, R. Wilson, A review of thermal and optical characterisation of complex window systems and their building performance prediction, Applied Energy. 222 (2018) 729–747. https://doi.org/10.1016/j.apenergy.2018.03.144.

[36] F. Chen, S.K. Wittkopf, Summer condition thermal transmittance measurement of fenestration systems using calorimetric hot box, Energy and Buildings. 53 (2012) 47–56. https://doi.org/10.1016/j.enbuild.2012.07.005.

[37] EN, 674: Glass in building – determination of thermal transmittance (U value) –Guarded hot plate method, 2011.

[38] EN, 675: Glass in building. Determination of thermal transmittance (U value). Heat flow meter method, 2011.

[39] EN, 1946-2: Thermal performance of building products and components. Specific criteria for the assessment of laboratories measuring heat transfer properties. Measurements by guarded hot plate method, 1999.

[40] EN, 1946-3: Thermal performance of building products and components. Specific criteria

for the assessment of laboratories measuring heat transfer properties. Measurements by heat flow meter method, 1999.
[41] JGJ/T 151-2008: Calculation specification for thermal performance of windows, doors, and glass curtain-walls (Chinese), 2008.
[42] National Fenestration Rating Council, ANSI/NFRC 100-2017 [E0A1]: Procedure for Determining Fenestration Product U-factors, National Fenestration Rating Council, 2016.
[43] ASHRAE, Fundamentals, 2017.
[44] Y. Fang, T.J. Hyde, F. Arya, N. Hewitt, R. Wang, Y. Dai, Enhancing the thermal performance of triple vacuum glazing with low-emittance coatings, Energy and Buildings. 97 (2015) 186–195. https://doi.org/10.1016/j.enbuild.2015.04.006.
[45] Y. Fang, T.J. Hyde, N. Hewitt, Predicted thermal performance of triple vacuum glazing, Solar Energy. 84 (2010) 2132–2139. https://doi.org/10.1016/j.solener.2010.09.002.
[46] W. Zhang, L. Lu, Overall energy assessment of semi-transparent photovoltaic insulated glass units for building integration under different climate conditions, Renewable Energy. 134 (2018) 818–827. https://doi.org/10.1016/J.RENENE.2018.11.043.
[47] W. Liao, S. Xu, Energy performance comparison among see-through amorphous-silicon PV (photovoltaic) glazings and traditional glazings under different architectural conditions in China, Energy. 83 (2015) 267–275. https://doi.org/10.1016/j.energy.2015.02.023.
[48] O. Aydin, Determination of optimum air-layer thickness in double-pane windows, Energy and Buildings. 32 (2000) 303–308. https://doi.org/10.1016/S0378-7788(00)00057-8.
[49] Berkeley Lab WINDOW, (n.d.). https://windows.lbl.gov/software/window.
[50] Lawrence Berkeley National Laboratory, https://windows.lbl.gov/software/igdb, (n.d.).
[51] R.E. Collins, T.M. Simko, Current status of the science and technology of vacuum glazing, Solar Energy. 62 (1998) 189–213. https://doi.org/10.1016/S0038-092X(98)00007-3.
[52] E. Cuce, S.B. Riffat, Aerogel-Assisted Support Pillars for Thermal Performance Enhancement of Vacuum Glazing: A CFD Research for a Commercial Product, Arabian Journal for Science and Engineering. 40 (2015) 2233–2238. https://doi.org/10.1007/s13369-015-1727-5.
[53] P.W. Griffiths, P.C. Eames, T.J. Hyde, Y. Fang, B. Norton, Experimental Characterization and Detailed Performance Prediction of a Vacuum Glazing System Fabricated With a Low Temperature Metal Edge Seal, Using a Validated Computer Model, Journal of Solar Energy Engineering, Transactions of the ASME. 128 (2006) 199–203. https://doi.org/10.1115/1.2188529.

[54] H. Manz, S. Brunner, L. Wullschleger, Triple vacuum glazing: Heat transfer and basic mechanical design constraints, Solar Energy. 80 (2006) 1632–1642. https://doi.org/10.1016/j.solener.2005.11.003.
[55] Y. Fang, P.C. Eames, B. Norton, T.J. Hyde, J. Zhao, J. Wang, Y. Huang, Low emittance coatings and the thermal performance of vacuum glazing, Solar Energy. 81 (2007) 8–12. https://doi.org/10.1016/j.solener.2006.06.011.
[56] ASHRAE, Fundamentals, 2001.